Preprints.org

Article

Groundwater Potential Zone Mapping to Understand the Sustainability of Springs in a Micro Watershed of Kosi River, Kumaun Lesser Himalaya, Uttarakhand, India

Puthiyottil Nijesh , Radha Dixit , Abhinav Patel , Abhinesh Kumar Singh , Anant Gautam , Raju Rai , Sury Kant Singh , Neeraj Pant , Meera Soman , Shive Prakash Rai [*]

Article

Groundwater Potential Zone Mapping to Understand the Sustainability of Springs in a Micro Watershed of Kosi River, Kumaun Lesser Himalaya, Uttarakhand, India

Puthiyottil Nijesh [1], Radha Dixit [1], Abhinav Patel [1], Abhinesh Kumar Singh [1], Anant Gautam [2], Raju Rai [1], Sury Kant Singh [1], Neeraj Pant [3], Meera Soman [4] and Shive Prakash Rai [1,*]

[1] Department of Geology, Institute of Science, Banaras Hindu University, Varanasi, Uttar Pradesh, 221005, India
[2] Department of Geology, Human Science, Sikkim University, Gangtok, Sikkim
[3] School of Engineering, Design and Built Environment, Western Sydney University, Australia
[4] Department of Geology, Anna University, Chennai, 600025, India
* Correspondence: sprai1966roorkee@gmail.com

Abstract: Springs play a significant role in maintaining hydrological balance in the mountain ecosystem. The communities living in the mountain tops rely entirely on spring water for their daily needs. In recent decades, spring water discharges have decreased drastically in the Himalayan regions and become seasonal. Remote sensing and geographical information system techniques have proved to be essential for understanding the sustainable development of groundwater, particularly where people rely solely on spring water in the mountainous regions of the Himalayas. This study employs the Analytical Hierarchy Process (AHP) to identify groundwater potential zones. It involves overlaying seven thematic layers concerning elements of physical features and land-use/land-cover of the region, using the weighted overlay toolbox in ArcGIS, with each layer being assigned a weight based on its importance. Based on the results, groundwater potential zones have been classified into five categories: poor, fair, good, very good, and excellent. The study found that poor groundwater potential zones cover 1.1% of the area, fair zones cover 27.8%, good zones cover 23.3%, very good zones cover 26.6%, and excellent zones cover 21.2% of the total area. The excellent to very good potential zones are associated with perennial springs that have higher discharge (4.30-30.92 l/m), lineaments, rainfall, forested land, and porous soils, favoring the potentiality of the springs. The fair and poor groundwater potential zones are associated with seasonal flowing springs, consisting of barren land, less rainfall, and low fracture density, which influence the potentiality of groundwater. The validation of the groundwater potential zones indicated an Area Under Curve (AUC) value of 0.88, which shows good agreement with observed spring water locations. The identified groundwater potential zones are valuable for prioritizing the area for the sustainable development of spring water. Particularly, it is helpful for policymakers and government bodies to be involved in developing strategies for sustainable water management at the micro-watershed level and safeguarding spring water resources using integrated watershed management in the headwater region of the Himalayas.

Keywords: springs; Khulgad micro watershed; AHP; lineaments; groundwater potential zone

1. Introduction

Groundwater proves to be an invaluable and priceless natural resource essential for various human activities, such as drinking water supply, industrial processes, and irrigation. Accounting for about 34% of the Earth's freshwater, it forms the largest freshwater resource in the world and is

immensely important for society [23,64]. Therefore, understanding the hydrological processes of this precious resource in a particular territory is necessary for supporting sustainable development.

The Sustainable Development Goal Six (SDG-6) of the United Nations aims to ensure universal access to clean drinking water, adequate sanitation, and improved hygiene, recognizing them as essential rights for all individuals by 2030 [66]. Setting up this kind of target is a dire necessity in the ongoing unsustainable practices in the world, which are not only leading to quantitative reduction of surface water but also have made direct use of this water harmful for human beings, inviting various diseases. Further, the pace of rapid modernization, industrialization, and intensive agricultural practices induced by high population growth has also led to the shortage and increase in the demand for clean drinking water in both rural and urban areas [18,85]. Organic and heavy metal contamination has accumulated in surface waterways due to excessive and uncontrolled use, lowering the water's quality. Meanwhile, global problems like drought and climate change have disastrously affected surface water, sometimes entirely destroying it.

These above-mentioned factors have led to humans' dependency on groundwater to satisfy their daily needs. Subsequently, the agriculture sector accounts for the largest utilization of the groundwater resource in the world, i.e., around 42% of the world's available groundwater, followed by household consumption for safe drinking water supply ranging between 25 % to 50% globally [65,71]. However, the proportion varies from country to country depending on the development level and the population's needs. In India, over 90% of people in rural areas and around 30% in urban areas rely on groundwater for drinking and domestic purposes, causing over-exploitation in certain regions of the country [5, 6, 78]. In rural Bangladesh, tube wells are the primary source of drinking and domestic needs [22]. In several rapidly developing sub-Saharan African nations, including Burkina Faso, the Central African Republic, South Sudan, Ethiopia, Chad, Nigeria, Somalia, and Uganda, groundwater serves as the primary water source for drinking around 70% to 90% of the local people [12,25]. In the United States, 38% of the population counts on groundwater for the purpose of drinking, sourced either from private wells or public systems, with self-supply wells catering to nearly 13% of the population [34,43]. In Nigeria, the dependency on groundwater is so high that only 20% of the Lagos population are provided with a piped utility water supply [15]. With respect to agricultural consumption, approximately half of India's irrigation activities rely on groundwater, making it one of the world's largest water consumers. In China, around 9 million hectares of land are irrigated using groundwater [30].

Around five million springs have been reported throughout India. Among those, around three million are in the Indian Himalayan regions and are experiencing depletion or seasonal fluctuation, attributed to diverse factors such as human interventions and the consequences of climate change [54,71]. The decline in spring water discharge can also be linked to rising temperatures, heightened rainfall intensity, altered temporal distribution, and a notable decrease in winter precipitation [58].

The drying of springs is increasingly recognized as a critical issue in the Himalayan region, with a notable decline in spring discharge being documented across various areas [71]. Research has highlighted severe water shortages due to the declining discharge of the springs, particularly during dry seasons [33,63]. A decline of over 30% in spring discharge over the past 30 years has been observed in Nepal's mid-hill region [8]. Additionally, about 50% of perennial springs in the Indian Himalayas have either turned out to be dry or become seasonal [53]. Similarly, reports from the Himalayan state of Uttarakhand indicate a significant reduction in spring flow [4,29]. In addition, the transformation of about 82% of the spring fed streams of the upper Kosi river from perennial to ephemeral over the last twenty-five years is a critical issue [57]. This drastic change has significantly reduced the lean flow of these rivers, creating serious challenges for the sustainability of the rivers and the communities that depend on them. Consequently, the local inhabitants are experiencing water shortages for drinking and irrigation, putting their livelihoods and the well-being of their livestock at risk.

The declining rate of ephemeral springs is notably faster than that of perennial springs in the Himalayan area [51]. Consequently, understanding and managing the Himalayan region's spring systems is challenging and crucial due to its accessibility. However, evaluating the capacity and

productivity of springs in the Himalayan region is essential to understanding groundwater availability [54]. The potential of springs indicates the probability of groundwater presence in regions with adequate water resources. In order to assess the potentiality of springs, the availability of groundwater has to be assessed, as it is the major source of water for the springs. For this purpose, remote Sensing (RS) and Geographic Information Systems (GIS) serve as efficient and cost-effective tools for generating valuable data on different thematic layers, aiding in the interpretation of potential groundwater zones [36,42,45–48]. RS techniques serve as a significant source of information regarding the correlation among slopes, landforms, land use, and lineaments. This data can act as an attribute in GIS and overlaid with additional datasets [46,72].

Recent studies have utilized various AI models to map groundwater prospect zones across different regions. In one study, Explainable Artificial Intelligence (XAI) was employed to assess fifteen groundwater conditioning factors using models like k-Nearest Neighbors (KNN), Neural Networks (NNET), Gradient Boosting Machines (GBM), Random Forest (RF), and Support Vector Machines (SVM). This study identified five zones with varying potential, ranging from very low suitability (14.95 to 300.24 km²) to very high suitability (969.49 to 1958.85 km²) [80]. The study in Kanchipuram district, Tamil Nadu, India, used Landsat data and seven thematic layers to delineate groundwater potential zones, validating their map with high accuracy using the ROC method [83]. A study conducted in Marathwada used frequency ratio (FR) and statistical index (SI) models across eight factors, with the SI model proving more effective for groundwater management and planning in the region [84]. These studies highlight diverse methodologies and their application in enhancing groundwater resource management strategies globally.

However, investigators have utilized RS and GIS techniques to recognize potential groundwater zones by employing diverse thematic layers and field-observed data to validate their findings [10,16,32,38,40,47,61]. However, the validations of groundwater potential zone maps with observed spring water discharge and perennial nature in a micro-watershed scale have not been explored sufficiently.

Therefore, the present study aims to delineate groundwater potential zones based on spring water discharge using RS and GIS techniques in the Khulgad micro watershed of the Kosi basin, Kumaun Lesser Himalaya. The demarcation of the potential zone mapping in a micro-watershed would be significantly useful for villagers, policymakers, and local government authorities to manage the potential zone of groundwater and conserve it at the micro-watershed level to meet the drinking water demand of the villagers.

2. Study Area

The Khulgad watershed is situated within the Kosi basin, located in the Lesser Himalayan terrain of India's Almora district, within Uttarakhand State (Figure. 1). Covering an area of approximately 33 km², the watershed's elevation ranges from 1080 m to 2140 m. The Syahidevi peak, locally known as the "water tower" of the Khulgad watershed, represents the highest point, contributing significantly to the area's water resources. The drainage pattern of the watershed trails a dendritic pattern, with some abrupt diversions noted in major drainage channels due to faults traversing the watershed [50]. Geomorphologically, the area comprises 24 types of fluvial, pluvial, and tectonic landforms [50,56].

The predominant land use/land cover in the area encompasses dense and semi-dense forests, primarily located in the southern and western parts of the watershed. Forested areas, mainly comprising oak and pine, cover approximately 52.2% of the total area, while barren land occupies 30.2%, agricultural land 13.7%, and urban areas 3.9%. The majority of the Khulgad micro watershed features shallow soil depths ranging from 25 to 55 cm, with sandy loam covering 50% of the area and the basin's outlet identified as sandy clay loam.

The annual average rainfall in the basin ranges from approximately 980 mm in August to around 8.2 mm in November. Summer monsoon rains contribute approximately 75% of the total annual rainfall. The Khulgad micro watershed falls within a cool temperate climate region, with an annual

average temperature of 20.3°C. The average maximum temperature was recorded as 26.7°C, and the minimum average temperature recorded was 15.3°C, respectively.

3. Hydrological and Geological Setting

The Khulgad watershed is situated within the northeast-dipping southern limb of the synclinal Almora Nappe, characterized by a thick folded sheet of Precambrian metamorphic rocks and associated granites [50]. Extensively studied by various researchers [20,35,50,67], the geological map reveals six lithological units within the basin.

Augen gneisses formation covers approximately 18.8% of the area, predominantly comprising sheared and fractured gneiss formations in the southwestern part of the watershed [50]. These gneisses pushed southward upon underlying schist and quartzite, have undergone extensive crushing, resulting in the development of secondary porosities that enhance permeability and form aquifers.

Garnetiferous mica schist, jointed quartzite, and friable quartzite, covering 18.8%, 28%, and 8% of the region respectively, from the underlying geological layers. Biotite schist and phyllite, constituting 15% and 8% of the watershed respectively, comprise the bottom layers (Figure 1b). Hydrogeologically, the area is characterized by aquifers of secondary porosity, primarily consisting of faults, fractures, and joints. Structural geology plays a crucial role in understanding the characteristics of springs and groundwater in the region. The Sitalakhet thrust passing over the Salla, Naula, and Dhamas schist and quartzite formations is particularly significant, as it contributes to the formation of secondary porosity, making this zone a potential aquifer. The gneissic rock in the thrust region has become highly permeable due to the formation of fractures and joints, underlain by gougy clay acting as an impermeable layer. Consequently, the thrust areas of Sitalakhet, Salla, Champa, Naula, and Syahidevi hills form clusters of springs. The discharge of these springs is primarily dependent on rainfall and its variability, with climate change emerging as a crucial factor influencing the quantity and quality of Himalayan springs, sustaining their flow throughout the year.
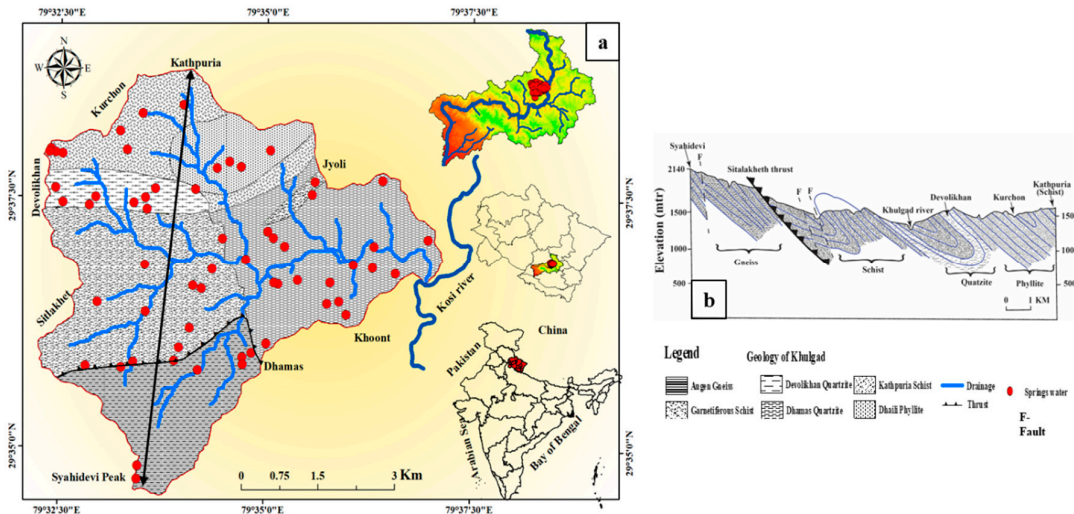

Figure 1. (a) Study area map of Khulgad micro watershed (b) geological cross section.

4. Materials and Methods

The remote sensing and GIS techniques are implemented to understand the spring water potential zone mapping in the micro watershed of Khulgad, for that a detailed methodology was developed (Figure 2). Various maps, such as lineament density, slope, drainage density, rainfall, and lithology map, were clubbed to create a groundwater potential map. The occurrence of groundwater is significantly influenced by hydrological conditions, which are primarily determined by these thematic layers. These layers serve as a dependable foundation for accurately predicting the groundwater potential of a given area [68].
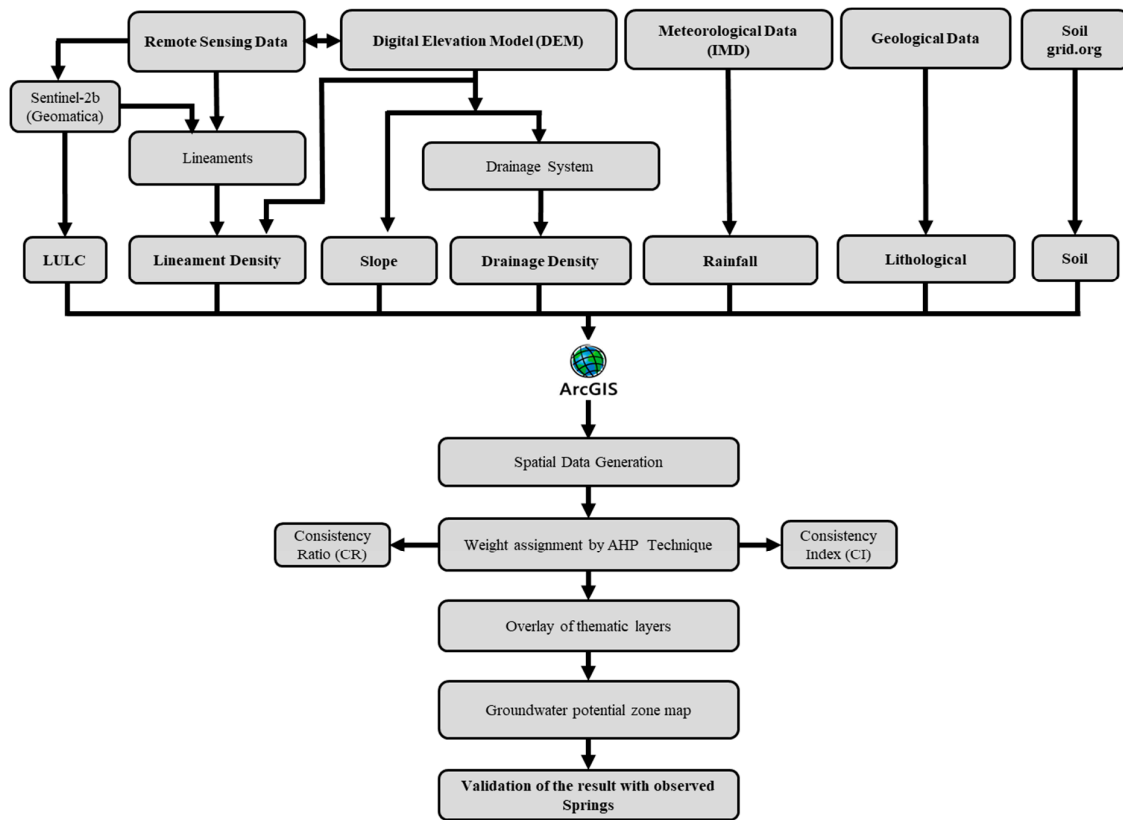
Figure 2. The methodology developed for the spring water potential zone mapping.

4.1. Preparation of Thematic Maps

4.1.1. Lineaments Extractions

The linear features are lineaments that are straight structural features visible on the surface of the earth, often referred to as significant "lines of landscape" [21]. The geological or geomorphic processes are the primary cause of these discontinuities [11]. The methodology employed in this study involves the analysis of various geospatial datasets to assess groundwater potential and hydrological characteristics within the study area. Firstly, linear features on the Earth's surface are identified using hillshade techniques based on the digital elevation model (DEM) with azimuth angles of 30°, 35°, 40°, and 45°. On the other hand, the linear features were automatically generated using Geomatica software with a sentinel-2B multispectral images dataset. In this, we utilize automated feature extraction tools available in Geomatica software to detect linear features in the imagery. These tools typically use algorithms based on edge detection, pattern recognition, or spectral analysis to identify potential lineaments. The lineaments generated from the remote sensing techniques were compared with an existing lineament map (NRSC-IRS-P6 LISS-3 FCC) of the area to validate the linear features in the study region.

The Lineament Density (LD) is calculated using Equation (1) by dividing the total length of all identified lineaments by the area of interest.

$$LD = \frac{\sum_{i=1}^{n} L_i}{A} \tag{1}$$

where ΣLi is the total length of the entire lineaments in km and the "A" is the grid area in km².

The total length of all lineaments (ΣLi) in kilometers is divided by the area of each grid in square kilometers to compute the lineament density value for all grids. The calculated value is then outlined at the corresponding center of the grid, and these values aid in generating the lineament density map using interpolation.

4.1.2. Drainage Density Analysis

Drainage density is a crucial metric used in hydrology to understand the distribution and characteristics of stream channels within a given area, typically measured in kilometers of channel length per square kilometer of drainage basin area (km/km²). It serves as an indicator of how closely spaced the stream channels are and provides insights into the nature of the surface materials. The drainage density is calculated based on the Equation (2).

$$DD = \frac{\sum_{i=1}^{n} D_i}{A} \tag{2}$$

where $\sum D_i$ is the overall stream length (km), and "A" is the area of the grid (km²).

Drainage density serves as a crucial indicator inversely related to permeability, thus holding significance in assessing groundwater potential [60]. In regions characterized by low drainage density, there is a higher potential for infiltration, as highlighted by [62], leading to the formation of favorable groundwater zones [13,32] compared to areas with high drainage density.

4.1.3. Slope and Land Use Analysis

The Slope, defined as the rate of change of elevation across a surface, finds a significant role in determining the movement of superficial water flow, primarily influenced by gravitational forces [14]. A slope map of the area under study was created from Advanced Land Observing Satellite Phased array–type L-band synthetic aperture radar (ALOS PASAR) DEM with 12 m resolution using ArcGIS 10.5 software. In this study, the slopes are characterized into five classes, very low, low, moderate, high, and very high in degree.

The land use/land cover (LULC) mapping holds great importance in remote sensing as it plays a crucial role in the development of groundwater resources. LULC directly influences various hydrogeological processes within the water cycle, such as infiltration, evapotranspiration, and surface runoff. Additionally, surface cover characteristics, like roughness, have a significant impact on discharge rates, with rougher surfaces generally leading to increased infiltration and reduced runoff.

For this study, land use and land cover are created based on the sentinel-2b optical imagery having 10m spatial resolution, each land use is created based on supervised classification with field verification.

4.1.4. Lithology and Soil Analysis

The lithology map was generated through field surveys and validated according to Rai, 1993 Ph.D. thesis. The study area encompasses various geological formations, including augen gneiss, garnetiferous schist, schist, quartzite, and phyllite. Each lithological unit possesses unique characteristics influencing its ability to facilitate water infiltration from precipitation. Consequently, specific weights were assigned to each lithology in the weighted overlay method in the arc GIS based on its infiltration capabilities.

The Soil map was downloaded from the (https://soilgrids.org/) website with a 200cm standard depth. The study area consists of three types of soil classes such as chernozems, leptosols, and luvisols. Among chernozems and luvisols, the leptosols are generally considered to be the most porous soil. Leptosols are characterized by their shallow depth and often have a high proportion of coarse fragments, such as gravel or rock fragments, within the soil profile. This coarse texture and shallow nature typically result in good drainage and high porosity, allowing water to infiltrate easily into the soil. Therefore, Leptosols tend to have higher porosity compared to Chernozems and Luvisols, making them more conducive to groundwater recharge and infiltration. Consequently, specific weights were given to each soil using the weighted overlay method in the arc GIS based on its infiltration capacity.

4.1.5. Rainfall Map Preparation

Rainfall being the primary source of recharge, as indicated by previous studies [32,60], governs the volume of water accessible for infiltration into the groundwater system, thus holding significant importance in this study's hydrological analysis [2]. Daily rainfall data spanning 14 years (2010–2023) were obtained from the Indian Meteorological Department (IMD) for all existing weather stations in and around the study area. The precipitation data is interpolated with two stations in the study area using Arc GIS 10.5.

4.1.6. Delineation of Groundwater Potential Zones

The groundwater potential zone map (GPM) for the study area was created by combining five different thematic maps using ArcGIS 10.5. The integration was conducted by summating the overall factors that influence groundwater. The following formula (3), derived from previous studies [27,37,47], was employed:

$$GPM=(MC1w \times SC1r) + (MC2w \times SC2r)$$
$$+ (MC3w \times SC3r) + (MC4w \times SC4r)+(MC5w \times SC5r) \tag{3}$$

Here, GPM represents the groundwater potential map, MC1 to MC5 denote the chief criteria from the thematic layer maps, (w) signifies the weight assigned to each thematic map, SC1–SC5 indicate the sub-criteria of each thematic layer map, and (r) represents the ranking of the sub-criteria.

4.2. Analytic Hierarchy Process (AHP)

The Analytic Hierarchy Process (AHP) was utilized to assign weights to the thematic layers according to their significance in influencing groundwater potential based on a literature review and expert opinions [76]. The expert opinions were gathered from hydrogeologists, geologists, geomorphologists, and local officials involved with groundwater resources through a questionnaire-based field survey. Each thematic layer map underwent classification, with ranks assigned to various features within each theme in Table 5 [9,31,75].

The major eigenvalue and consistency index within the Analytic Hierarchy Process (AHP) encompass judgmental uncertainty [76]. Therefore, Table 1 provides a pairwise comparison matrix for the thematic layers with strength assessments. Additionally, Table 2 calculates the normalized pairwise matrix for criteria weightage to calculate the consistency index (CI) and consistency ratio (CR). The consistency index (CI) was utilized to assess the accuracy of pairwise comparisons, while the consistency ratio (CR) was employed to validate judgment consistency (Table 3). The CR controls the balance at which weights are assigned in Equation (5). It is essential for the weights to be as accurate as possible and not be overestimated or underestimated, given that they are determined by field surveys and literature reviews. The acceptable CR level is < 0.10. However, the saaty's provides a measure of consistency known as the Consistency Index (CI), calculated using Equation (5). The consistency indices of RI values in Table 4 were 1.32 for the seven factors.

$$CI = \frac{\lambda max - n}{n - 1} \tag{4}$$

$$CR = \frac{CI}{RI} \tag{5}$$

Where the λmax was the eigenvalues of the consistency index, n was the number of factors used. The Equation (5) was calculated with the help of Equation (4) Where the CR was the consistency ratio and the CI was the consistency index, RI was the ratio index. The consistency index (CI) was calculated as 0.05 which is less than 0.1. The consistency ratio was found that 0.037 which is acceptable for the consistency judgement.

Table 1. Comparative matrix of the seven thematic layers.

Factors	Rain	GLG	SL	DD	LULC	LD	Soil
Rain	1	3.0	3.0	5.0	5.0	5.0	7.0
GLG	0.3	1	3.0	3.0	5.0	5.0	5.0
SL	0.3	0.3	1	1.0	3.0	3.0	5.0
DD	0.2	0.3	1.0	1	1.0	2.0	3.0
LULC	0.2	0.2	0.3	1.0	1	1.0	3.0
LD	0.2	0.2	0.3	0.5	1.0	1	1.0
Soil	0.1	0.2	0.2	0.3	0.3	1.0	1

Table 2. Normalized matrix various seven thematic layers.

Factors	Rain	GLG	SL	DD	LULC	LD	Soil	Criteria Sum	Criteria weight	Weight%
Rain	0.42	0.57	0.34	0.42	0.31	0.28	0.28	2.62	0.4	37.4
GLG	0.14	0.19	0.34	0.25	0.31	0.28	0.20	1.71	0.2	24.4
SL	0.14	0.06	0.11	0.08	0.18	0.17	0.20	0.94	0.1	13.4
DD	0.08	0.06	0.11	0.08	0.06	0.11	0.12	0.62	0.1	8.9
LULC	0.08	0.04	0.04	0.08	0.06	0.06	0.12	0.48	0.1	6.9
LD	0.08	0.04	0.04	0.04	0.06	0.06	0.04	0.36	0.1	5.1
Soil	0.06	0.04	0.02	0.03	0.02	0.06	0.04	0.27	0.0	3.9

Table 3. Consistency index of eigenvalue.

Factors	Rain	GLG	SL	DD	LULC	LD	Soil	Weight sum	Criteria weight	λ
Rain	0.37	0.73	0.41	0.45	0.34	0.26	0.26	2.82	0.37	7.6
GLG	0.12	0.24	0.41	0.27	0.34	0.26	0.19	1.83	0.24	7.5
SL	0.12	0.08	0.14	0.09	0.21	0.15	0.19	0.98	0.14	7.2
DD	0.07	0.08	0.14	0.09	0.07	0.1	0.11	0.66	0.09	7.3
LULC	0.07	0.05	0.05	0.09	0.07	0.05	0.11	0.49	0.07	7.2
LD	0.07	0.05	0.05	0.05	0.07	0.05	0.04	0.38	0.05	7.3
Soil	0.05	0.05	0.03	0.03	0.02	0.05	0.04	0.27	0.04	7.2

Factors GLG= Geology; SL= Slope; DD=Drainage density; LULC= Land use and Land Cover; LD= Lineament density.

Table 4. Saaty's consistency indices of random value.

N	1	2	3	4	5	6	7	8	9
RI	0	0	0.58	0.89	1.12	1.24	1.32	1.41	1.45

4.3. Validation of the Analysis

The validation process of the data involves several steps to ensure its accuracy and reliability. For the lineament data, field observations play a crucial role in validating the detected features. Field survey was carried out to verify the presence and characteristics of lineaments identified through remote sensing techniques. Additionally, lineament maps are utilized as reference documents to cross-validate the detected lineaments with known geological features and structures. This comprehensive validation approach helps confirm the accuracy of the lineament data and enhances confidence in its interpretation.

Regarding the groundwater potential map, validation is primarily conducted through field observations of observed spring discharge. Field surveys are conducted to locate and document perennial and ephemeral springs within the study area (Figure 3). The locations of these observed springs are then compared with the groundwater potential map to assess their reliability in

categorizing areas with high groundwater potential. If the mapped groundwater potential zones correspond well with the observed spring with higher discharge in the field, it provides validation of the accuracy and effectiveness of the groundwater potential map. On the other hand, the groundwater potential zone map was assessed using the Receiver Operating Characteristic (ROC) curve and the Area Under the Curve (AUC) metrics. The ROC curve, which ranges from 0.5 to 1.0, is used to estimate the model's accuracy. Specifically, the AUC value stipulates a single measure of overall model performance. An AUC value of 0.5 indicates that the model performs no better than random chance, while values closer to 1.0 indicate higher model accuracy. It plots the True Positive Rate (TPR) against the False Positive Rate (FPR) Equations (6) and (7) [41,49]. This validation process helps ensure that the map provides reliable information for groundwater resource management and decision-making purposes.

$$TPR = \frac{True\ Positives}{True\ Positives + False\ Negatives} \tag{6}$$

$$FPR = \frac{False\ Positives}{False\ Positives + True\ Negatives} \tag{7}$$

This validation process helps ensure that the map provides reliable information for groundwater resource management and decision-making purposes.

Table 5. Weights, both assigned and normalized, are attributed to various features within seven thematic layers.

Themes	Feature/ Classes	Category of Groundwater Potential Storage	Rank assigned	Weight %
Land use/land cover (LULC)	Dense forest	Very High	5	
	Semi dense forest	Very High	5	
	Agricultural land	High	4	
	Buildup area	Low	2	6.9
	Road	Very low	1	
	Barren land	Moderate	3	
	Waterbody	High	4	
Lineament density (km²)	0-1.3	Very low	1	
	1.3-2.5	Low	2	
	2.5-3.7	Moderate	3	5.1
	3.7-5.0	High	4	
	5.0-6.5	Very high	5	
Drainage density (km²)	0-2.0	Very High	5	
	2.0-4.0	High	4	
	4.0-6.0	Moderate	3	8.9
	6.0-8.0	Low	2	
	8.0-10.0	Very Low	1	
Slope (degrees)	0-10	Very high	5	
	10-20	High	4	
	20-30	Moderate	3	13.4
	30-40	Low	2	
	40-60	Very low	1	
Geology	Gneiss	Low	1	
	Schist	Low	1	
	Phyllite	Moderate	3	24.4
	Garnetiferous schist	Low	2	
	Quartzite	Very low	1	

Soil	Leptosol	Very High	5	
	Luvisol	Moderate	3	3.9
	Chernozems	Moderate	3	
Rainfall (mm)	956-959	Very low	1	
	960-962	Low	2	
	963-966	Moderate	3	37.4
	967-969	High	4	
	970-973	Very high	5	

Figure 3. a-e. Shows the water crisis and drying issues of springs (locally called Naula).

5. Results

5.1. Soil Map

The study area exhibits three types of soil classes, namely chernozems covering 15.3km², leptosols covering 17.4km², and luvisols covering only 0.17km². Among these three types, leptosols are considered to be the most porous. They are characterized by their shallow depth and high proportion of coarse fragments, such as gravel or rock fragments within the soil profile. This results in good drainage, high porosity, and easy water infiltration into the soil. Consequently, 53% of the study area is covered by leptosols in the northern half of the study area, making them more conducive to groundwater recharge and infiltration. On the other hand, chernozems cover around 47% of the area, mainly in the southern parts, and luvisols are present in a very small area, around 0.5% in certain pockets in northcentral and northeast (Figure 4 and Table 7). Therefore, understanding the soil types is essential for understanding the groundwater potentiality of the study area.
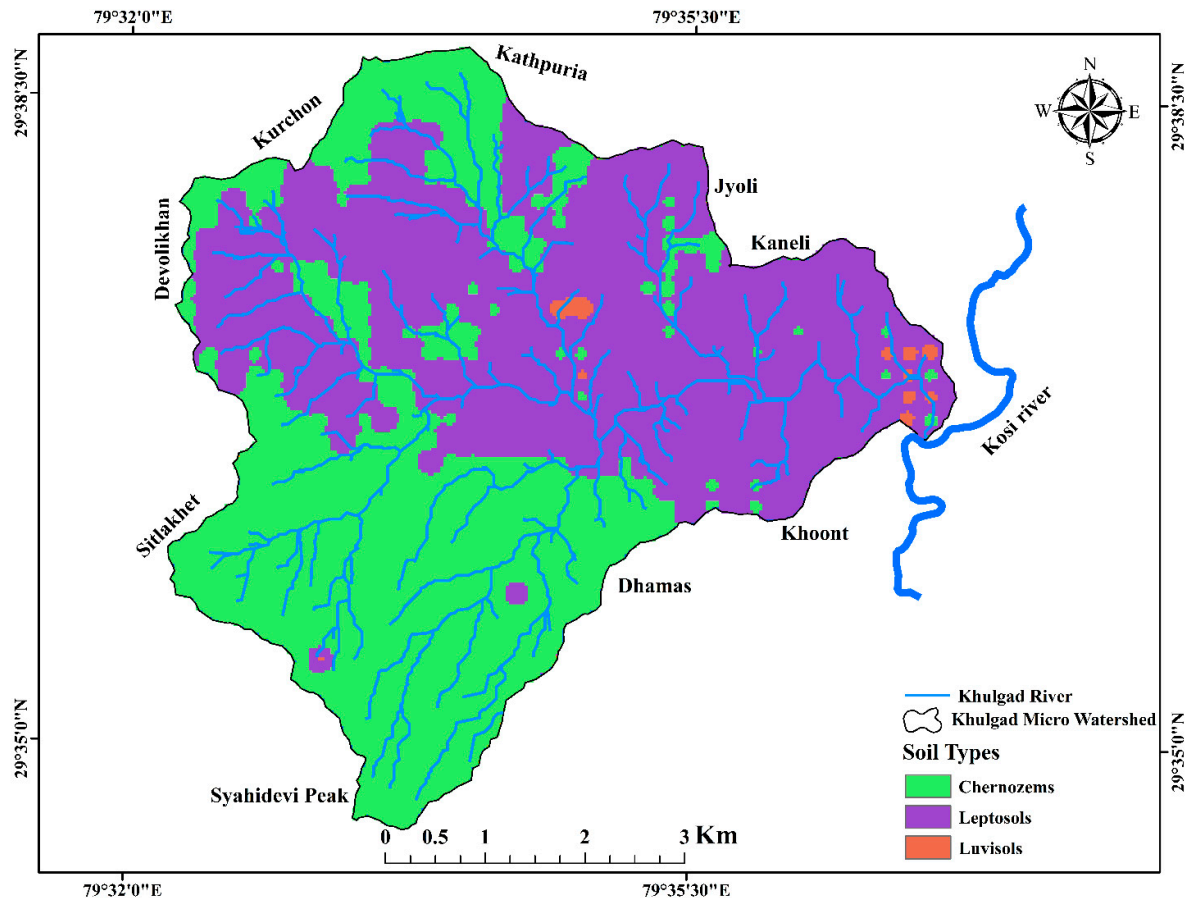
Figure 4. Soil type map of the study area.

5.2. Lithology Map

The lithology map delineates several geological formations within the study area, including Augen gneiss covering an area of 5.4 km², Devolikhan quartzite spanning 2.04 km², Garnetiferous schist extending over 9.29 km², Dhaili phyllite occupying 2.68 km², Dhamas quartzite encompassing 9.02 km², Muscovite schist covering 0.31 km², and Kathpuria schist spanning 0.77 km² (Figure 5 and Table 7). These geological formations exhibit secondary porosity, facilitating the transmission of groundwater (Figure 10). The southwestern region of the area hosts the gneissic rock, characterized by chernozems (organic black soil) in the topsoil layer and dense and semi-forested vegetation cover, suggesting a favorable environment for groundwater availability. Garnetiferous schist predominates below the gneissic rock, which covers 28.2% of the study area with a rank of two due to its low porous and permeable nature; however, these rocks have higher secondary porosity, such as fractures, which can hold a good amount of water [50]. While Dhamas quartzite is the second most abundant rock type found in the eastern part of the region covering an area of 27.4% with very low porosity nature, on the other hand this area stabilizes the groundwater potentiality by the influence of secondary porosity, soil type, and land use.
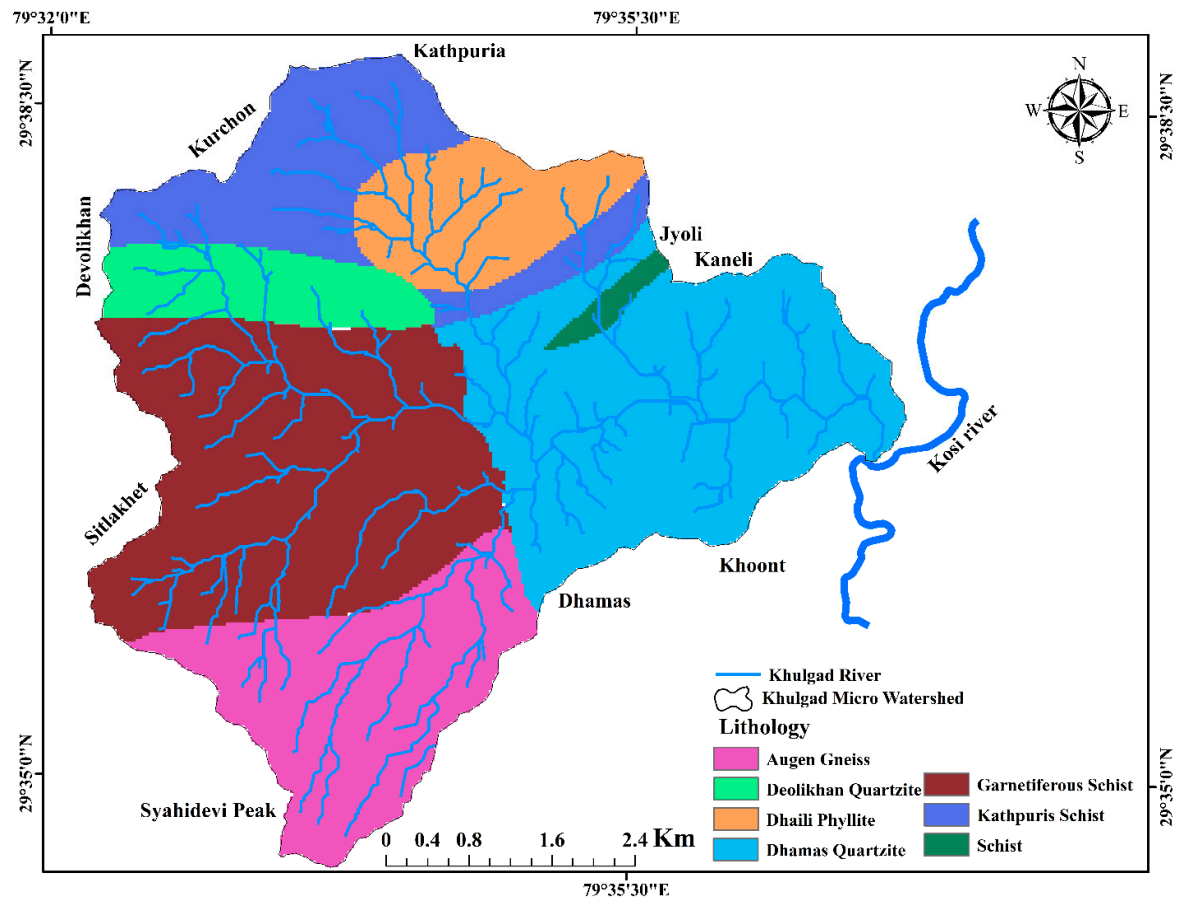
Figure 5. Lithological map of the Khulgad watershed.

5.3. Lineament Density Map

The lineament density map of the Khulgad micro watershed has been grouped into five categories (Table 5), each representing the intensity of fractures or joints in the region (Figure 6). Rank one indicates a very low intensity of lineaments, while rank five represents a very high intensity. The smallest area covered is rank one with 8.66 km², followed by rank two with 5.9 km². Rank three has the highest area of coverage with 9.94 km², while rank four constitutes 5.55 km² (Table 7). The lineament density between ranks three and five has a higher chance of groundwater potential than one and two. However, it is completely dependent on the aquifer properties. Based on the potentiality of groundwater, the very high groundwater potential area covers around 8.8% of the total area, the high groundwater potential area covers about 16.8% of the total area, the moderate groundwater potential area covers approximately 30.1%, the low groundwater potential area covers 17.9%, and the very low groundwater potential area covers around 26.3% of the total study area.
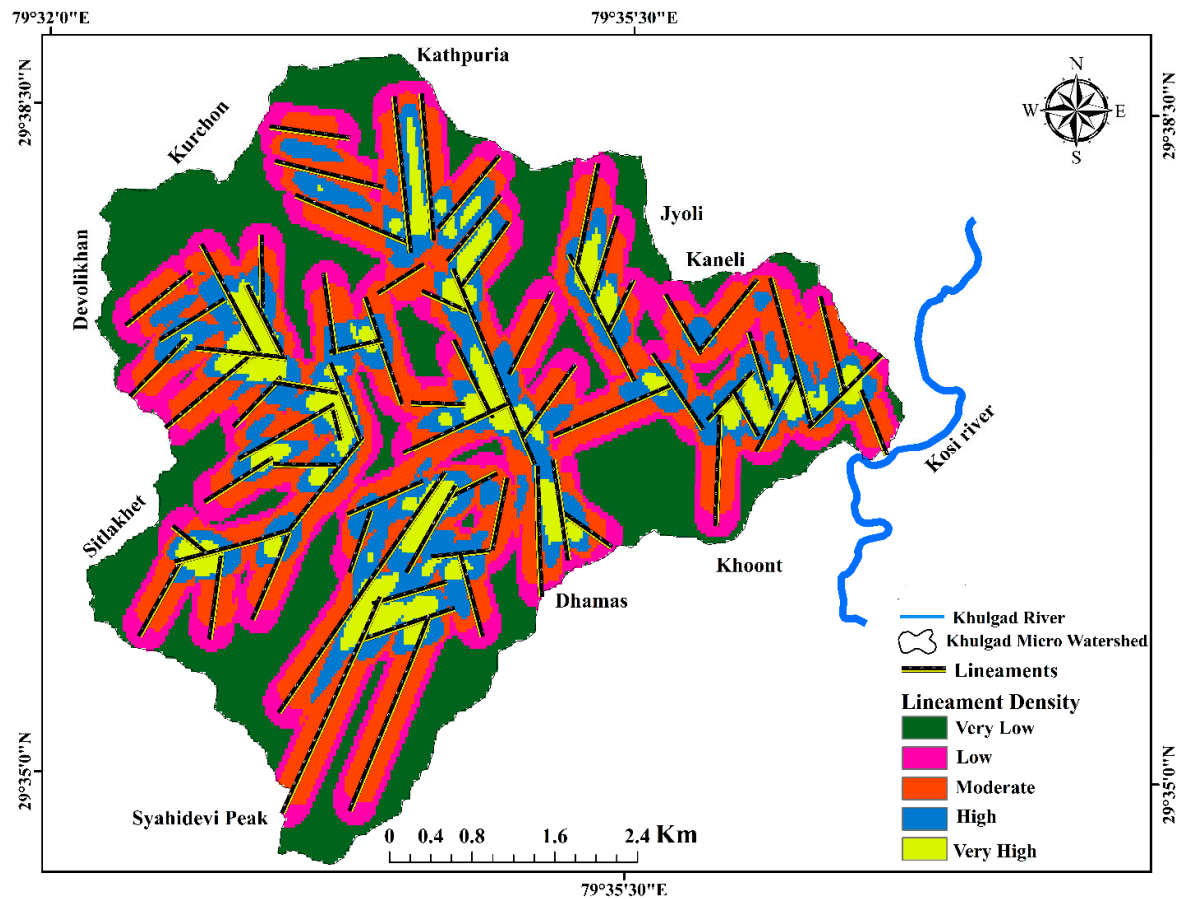
Figure 6. Lineament density map of the study area.

5.4. Drainage Density Map

The drainage density of the watershed is determined by the availability of a maximum number of channels present in that area. In this particular study, the drainage density has been categorized into five ranks based on the density of the drainages, similar to the lineament density (Figure 7). The highest drainage density has been given to rank one, covering an area of 10 km², while the least drainage density area has been assigned to the weighted rank of five, consisting of an area of 2 km². However, 74.5% of the study area shows evidence of moderate to very high groundwater capability, while the remaining 25.5% indicates very low to low groundwater potential based on the density of the drainage (Table 7). The majority of the groundwater potential zone is located in the southwestern and central parts of the watershed.

Figure 7. Shows the drainage density map of the study area.

5.5. Land Use and Land Cover (LULC)

The map of LULC comprises seven different categories of land use, which are dense forest, semi-dense forest, agricultural land settlements, roads, barren land, water bodies, and built-up areas. Each type of land use has been given a weightage based on its capacity to retain groundwater (Table 5). The highest weighted ranks of five have been assigned to dense and semi-dense forests, respectively, as they have the maximum capacity to store water for infiltration and significantly contribute to groundwater recharge. On the other hand, the lowest ranking has been given to roads and barren land, as they hardly provide a suitable environment for water infiltration, and most of the water entering its surface area drains away as surface run-off. The LULC analysis of the study area revealed that the total area covered by forested is 17.1 km²; out of which 2.1 km² is dense forest, 3.3 km² is agricultural land, 10.3 km² is barren land, 0.6 km² is water body, 1.2 km² is roads, and 0.4 km² is built-up area (Table 7). However, the entire 17.2 km² area of forested land in the southwestern part of the study area shows great potential for groundwater (Figure 8).
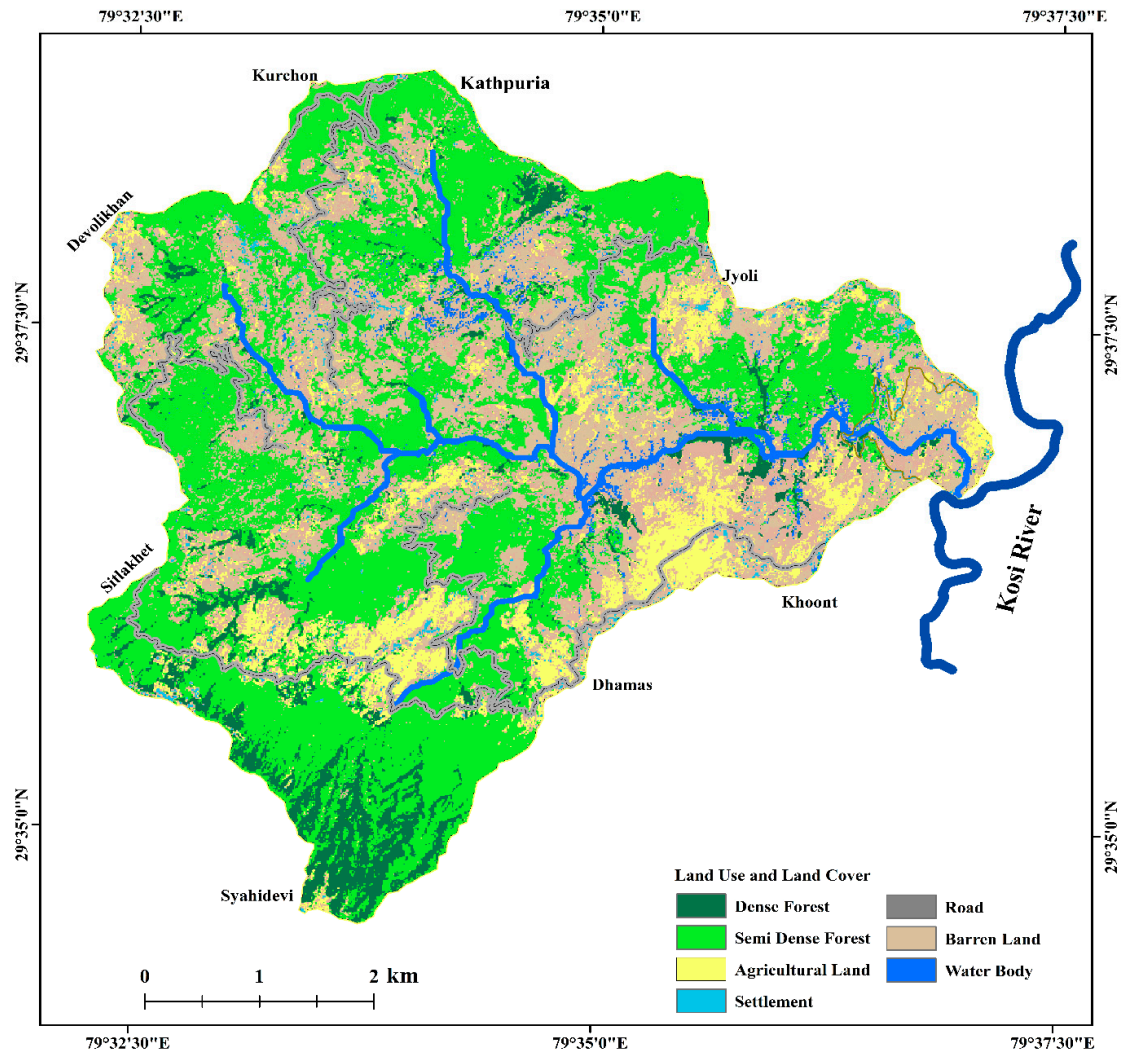
15

Figure 8. Land use and land cover map of Khulgad micro watershed.

5.6. Slope Map

The slope forms a crucial topographic parameter that indicates how steep or gentle the terrain is [14]. The spacing between the contours can help determine the slope. The contours are closely spaced in a terrain, indicating a steeper slope, whereas broadly spaced contours suggest a gentle slope. In an elevation output raster, each cell is assigned a slope value. Lower slope angle values signify flatter terrain, while higher slope angle values denote steeper areas. The slope is measured by determining the maximum rate of change in elevation from each cell to its neighboring cells. These slope values can be expressed either in percentages or degrees and can be calculated in both vector and raster formats.

The slope analysis reveals that the slope of the relief features decreases from the northern part to the central and eastern parts of the area, with slopes ranging from 0° to 10° in both flat and mountainous regions, respectively. In areas with nearly level slopes (0-10 degrees), surface runoff is slow, giving more time for rainwater to infiltrate and percolate, thus creating zones with good groundwater potential. Conversely, in regions with steep slopes (31-60 degrees), runoff is rapid, reducing the time rainwater stays on the surface and consequently bringing about lower infiltration rates. This results in poor groundwater potential, particularly in the northeastern part of the study area, which is marked by high to very high slopes. The slope map is categorized into five distinct classes (Figure 9).
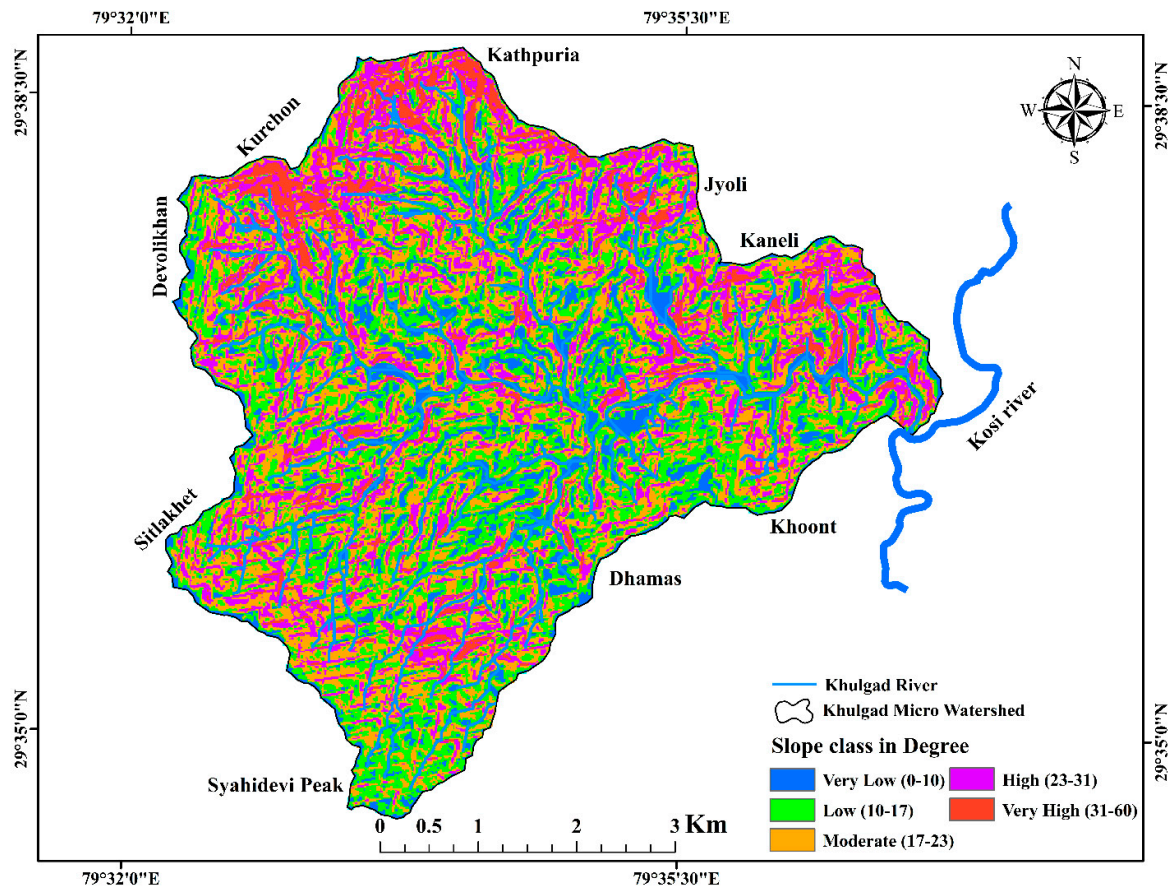
Figure 9. Slope map of Khulgad micro watershed.

5.7. Rainfall Map

The map shows the annual average rainfall of the study area (Figure 9), with a weighted rank of one to five assigned for low to high rainfall. The highest rainfall is recorded in the southwestern part of the study area, with an annual average of 970 to 980mm. Hence, this zone has been attributed to the highest weighted rank, i.e., 5 (Table 5). The lowest annual average rainfall has been recorded in the eastern part of the study area, i.e., 960mm only, leading to comparatively lesser water availability for groundwater recharge. Hence, the lowest weighted rank of 1 has been assigned to this zone for the current analysis. The spatial distribution of rainfall pattern in the study area reveals the highest rainfall (973 mm) occurring in the southwestern parts of the study area with the highest potential of groundwater recharge, and this trend decreases in the north and east directions (Figure 10).
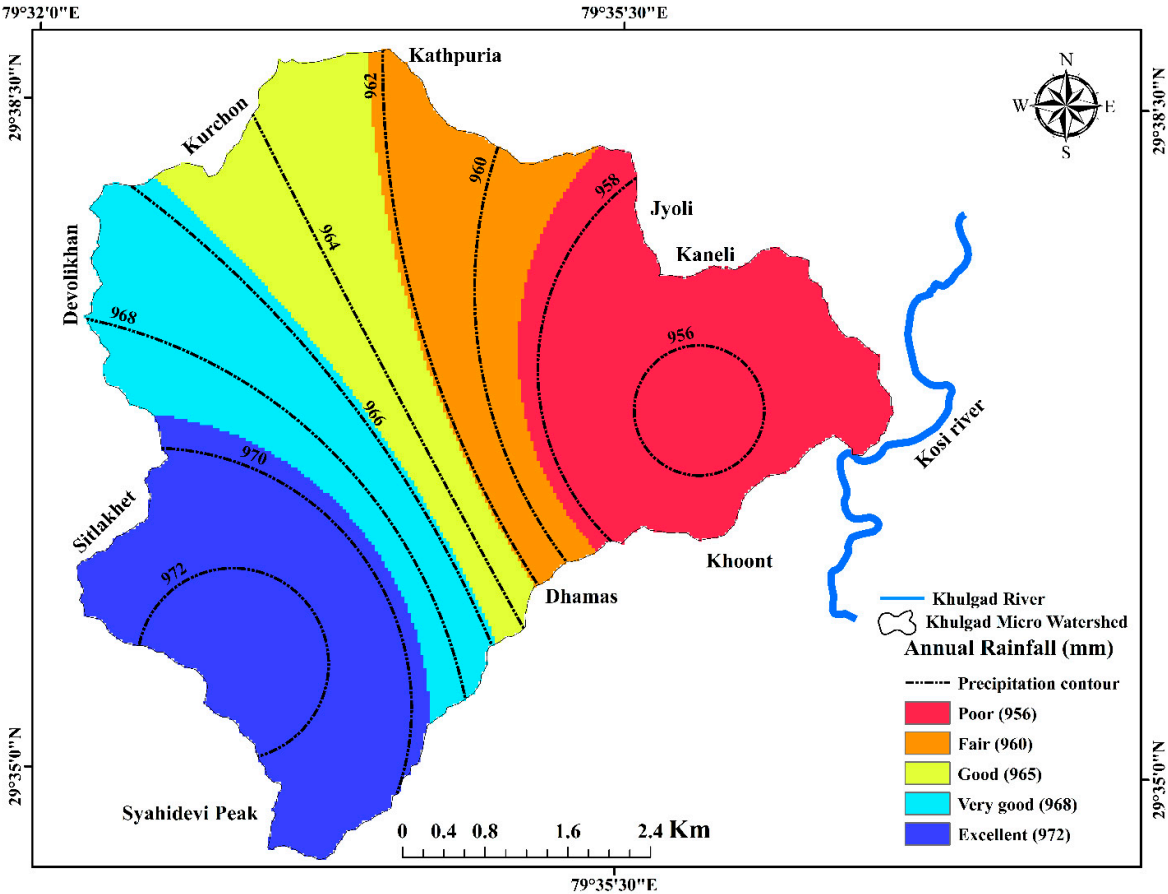
Figure 10. Rainfall map of the micro watershed of Khulgad.

5.8. Validation of Groundwater Potential Zones

The potential groundwater zone has been verified through field observations of the springs and the existing lineament map (NRSC-IRS-P6 LISS-3 FCC) in order to validate the groundwater potential zones in the study area. Measurements of the discharge of spring water were taken in the field to validate the groundwater potential zone in the area.   50% of the perennial springs of the study area are located in the excellent and very good groundwater potential area, 15% of the springs are in the good groundwater potential zone, and the remaining 35% are in the fair to poor groundwater potential area (Table 6). Among the 35% and 10% are in the poor groundwater potential zone, with conclusive evidence that ephemeral and low discharge springs are clustered together. Apart from that, the springs are primarily connected to lineament features or fractures, and those with higher discharge are more closely associated with these features (Figure 11). The springs that appear seasonal are mostly found in areas with fair to poor groundwater potential zones covering around 29% of the study area. The remaining 71 % of the study area is in the good to excellent groundwater potential zone. This indicates that the analysis made in this study is supported by the available field evidence. The AUC 0.88 value indicates that the model performance is good with the observed spring water in the study area (Figure 12).

Table 6. Classification of groundwater potential zone and the respective area.

Potential zones	Area (Km²)	%Area
Poor	0.36	1.1
Fair	9.18	27.8
Good	7.69	23.3

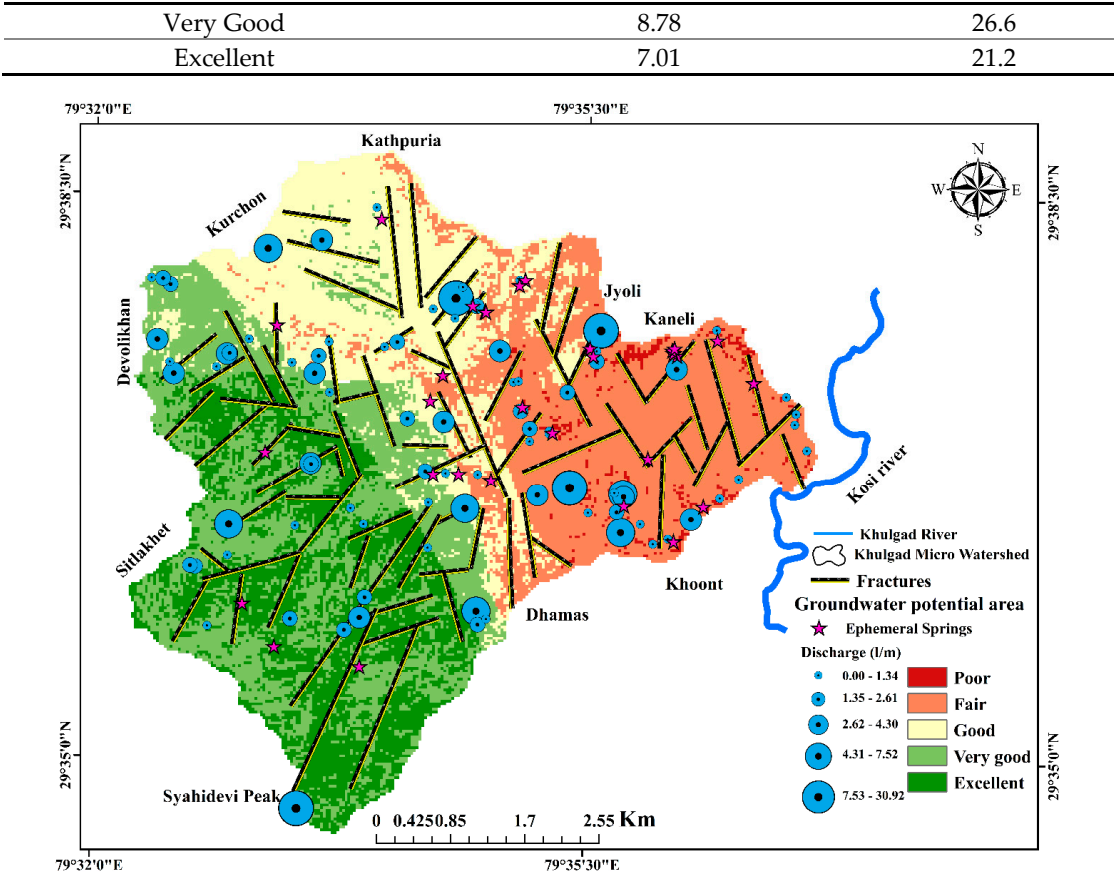| Very Good	8.78	26.6
Excellent	7.01	21.2

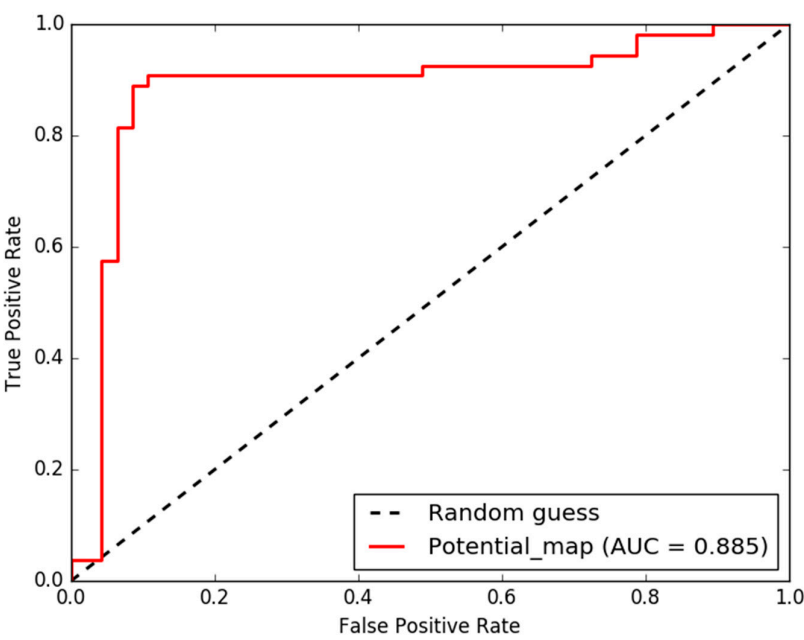**Figure 11.** Groundwater potential zone map with Spring discharge.

Figure 12. The model validation using ROC curve with observed spring and potential map.

Table 7. Various thematic layers show the percentage of groundwater potential area and its respective rank.

Themes	Potentiality for Groundwater Storage	Assigned Rank	% Area
Land use and land cover	Very High (Dense forest)	5	45.1
	Very High (Forested land)	5	6.5
	High (Agricultural land)	4	19.0
	Low (Buildup area)	2	10.0
	Very low (Road)	1	1.4
	Moderate (Barren land)	3	16.3
	High (Water body)	4	1.7
Lineament density (km/km²)	Very low	1	26.3
	Low	2	17.9
	Moderate	3	30.1
	High	4	16.8
	Very high	5	8.8
Drainage density (km/km²)	Very High	5	25.0
	High	4	26.2
	Moderate	3	23.3
	Low	2	19.2
	Very Low	1	6.3
Slope (degrees)	Very high	5	13.9
	High	4	29.0
	Moderate	3	30.3
	Low	2	20.0
	Very low	1	6.9
Geology	Moderate (Augen gneiss)	3	16.4
	Low (Schist)	2	0.9
	Moderate (Daili phyllite)	3	8.1
	Low(Garnetiferous schist)	2	28.2
	Very low (Quartzite)	1	27.4
	Very low (Devolikhan quartzite)	1	6.2
	Kathpuria schist	2	10.3
Soil	Very High (Leptosol)	5	52.8
	Moderate (Luvisol)	3	0.5
	Moderate (Chernozems)	3	46.5
Rainfall (mm)	Very low	1	25.2
	Low	2	14.9
	Moderate	3	17.4
	High	4	18.4
	Very high	5	24.0

6. Discussion

The identification of groundwater potential zones helps to understand the availability of groundwater resources in a specific area. The parameters for mapping depend on the physical conditions of the region. In this study, seven thematic layers, such as slope, lineament density, lithology, drainage density, rainfall, soil, and land use land cover, were prepared to identify the groundwater potential zones [3,7,26,54,69,70,74]. Each thematic layer was assigned a weight from a 1-5 scale, the 1 indicates low value, and 5 indicates high value based on the hydrological conditions of the area [54].

The rainfall is one of the primary inputs for the mountainous regions. Hence, the relationship between rainfall and groundwater potential zone mapping is a crucial aspect, especially the high rainfall was concentrated in the southwestern part of the study area, varying from 970 to 973 mm. However, it's important to note that groundwater potential is not solely determined by rainfall, other factors, such as the water-holding capacity of the aquifer material, lineaments, geology, slope, soil, land use, and drainage density also play significant roles [75,79].

The lithology and secondary porosity directly impact the water-holding capacity of rocks in the study area [56]. The field observations confirm that the gneissic rock in the southwestern part of the study area shows the highest amount of secondary porosity. Therefore, it has been assigned 5, the highest rank. The linear features in the watershed suggest that hard rock terrains transmit more water due to the presence of inter-connected secondary porosity [17,39,79]. For this study, lineaments are digitized from satellite imagery (IRS-P6 LISS-3 FCC). However, both digitized lineaments and field-surveyed lineaments were used to understand the groundwater potentiality of the area.

In the Khulgad micro watershed, the steep slopes prevent the infiltration of rainfall into the aquifer system, particularly in areas with a very high degree of slope (>30 degrees), representing lower groundwater potential compared to other regions. Conversely, the southwestern part of the study area, characterized by lower slopes (0-10°, 10-17°, 17-23°), exhibits the highest groundwater potential. However, the northern part of the watershed (Kathpuria, Kurchon, Kaneli) shows higher steep slopes >30 degrees, indicating less groundwater potential, which was ranked as 1 and 2. Similarly, other researchers have explored the impact of slopes on groundwater potential in different terrains [52,55]. These studies revealed that steep slopes (>30 degrees) were linked to lower groundwater potential because of quick runoff and limited infiltration. On the other hand, slopes less than 15 degrees were associated with higher groundwater recharge [55].

In the study area, soil has been ranked based on the texture and water-holding capacity, and the highest rank-5 has been assigned to the leptosol soil, and the moderate rank of 3 was assigned to the luvisol and chernozems [86]. Similarly, for LULC, the highest rank of 5 was assigned to the forested land and low to very low for the buildup regions and roads in the study area [87]. The drainage density of the watershed is also important to understand groundwater availability. The drainage density has been ranked 5 for very low drainage dense regions due to the less runoff and higher chance of infiltration, and the rank 1 has been assigned to high drainage dense regions due to the sudden runoff [79,82].

The current study utilized seven thematic layers integrated using the Analytical Hierarchy Process (AHP). However, the AHP has some limitations due to the subjective nature of assigning weights to the layers. To address this, we conducted an extensive literature review and field observations and sought expert opinions to determine the weights for each thematic layer. The consistency of the result can be checked by the consistency ratio (CR) value for the analysis. The CR value <10% (0.1) is accepted, and the weight and rank assigned to the parameters are justified and suitable for the AHP analysis [75,77]. In the present study, the CR value is 4% for seven parameters, which suggests the pairwise comparison is consistent.

The validation of the groundwater potential zones using RS and GIS with field observed data is always challenging in the absence of observed well yield and other available water resources information, particularly in the Himalayan regions [54,60]. In the current study, we followed similar approaches to substantiate groundwater potential zones. The occurrence, distribution, discharge of the spring, and density of the perennial springs are used to validate the groundwater potential area (Figure 12). The validation revealed that about 50% of the perennial springs in the study area are located in excellent and very good groundwater potential zones. Geologically, this part of the basin is made up of fractured rocks of Gneiss and Quartzite, which is covered with thick soil and densely forested land. All these conditions are favorable for the high recharge in this part of the basin. Additionally, the ROC curve was employed further to justify the groundwater potential areas. Similarly, ROC curve methods were used by various researchers to validate the groundwater potential zone mapping [19,44].

This study has significant importance for local villagers regarding better groundwater utilization. This study provides a valuable resource for targeted water resource management and strategic planning. The policymakers can use this information to prioritize regions for groundwater extraction, implement sustainable water usage practices, and plan for infrastructure development, such as rainfall harvesting structures and spring water storage tanks to reduce the runoff. Additionally, the identified low potential zones in the eastern parts of the study area allow for better drought preparedness and management strategies, ensuring that water resources are allocated efficiently during periods of scarcity. Overall, this study helps policymakers and local villagers for implementing long-term strategies for sustainable water management.

7. Conclusions

The Khulgad micro-watershed in the Kosi basin has been analyzed to identify potential groundwater available zones. The results show that 48% of the area in the southwestern part of the Khulgad watershed has excellent to very good groundwater potential, preeminently in the highly forested, low slope areas with a higher frequency of fractures where 76.9% of the springs are perennial. The lineaments are mostly found in areas with very good to excellent groundwater potential, and the springs found along these lineaments are perennial with excellent discharge. However, 23.1% of the seasonal or dried-up springs match with poor to fair groundwater potential zones due to the steep slope, less forest cover, and more barren land, triggering the low groundwater potential in the southeastern part of the study area. The groundwater potential modeling with the AHP method has predicted values with an 88% accurate ROC curve, indicating good model performance is valid based on observed springs. The study will be valuable for policymakers and stakeholders in sustaining spring water and groundwater at the village level of the Khulgad micro-watershed through engineering and biological interventions in the low groundwater potential zone. Overall, the study reveals that it can be replicated in a similar micro-watershed of the Himalayas.

References

1. Abdelkareem, M., Abdalla, F., Alshehri, F., & Pande, C. B. (2023). Mapping Groundwater Prospective Zones Using Remote Sensing and Geographical Information System Techniques in Wadi Fatima, Western Saudi Arabia. Sustainability, 15(21), 15629.
2. Adiat, K. A. N., Nawawi, M. N. M., & Abdullah, K. (2012). Assessing the accuracy of GIS-based elementary multi criteria decision analysis as a spatial prediction tool–a case of predicting potential zones of sustainable groundwater resources. Journal of Hydrology, 440, 75-89.
3. Adnan, N. A., & Atkinson, P. M. (2011). Exploring the impact of climate and land use changes on streamflow trends in a monsoon catchment. International journal of climatology, 31(6), 815-831.

4.   Agarwal A, Bhatnagar NK, Nema RK, et al. (2012) Rainfall dependence of springs in the Midwestern Himalayan hills of Uttarakhand. Mountain Research and Development 32(4): 446-455. https://doi.org/10.1659/MRD-JOURNAL-D-12-00054.1.

5.   Patel, A., Rai, S. P., Akpataku, K. V., Puthiyottil, N., Singh, A. K., Pant, N., ... & Noble, J. (2023). Hydrogeochemical characterization of groundwater in the shallow aquifer system of Middle Ganga Basin, India. Groundwater for Sustainable Development, 21, 100934.

6.   Ali, S., Fakhri, Y., Golbini, M., Thakur, S. K., Alinejad, A., Parseh, I., ... & Bhattacharya, P. (2019). Concentration of fluoride in groundwater of India: a systematic review, meta-analysis and risk assessment. Groundwater for Sustainable Development, 9, 100224.

7.   Al-Shabeeb, A. R., Hamdan, I., Al-Fugara, A. K., Al-Adamat, R., & Alrawashdeh, M. (2023). Spatial mapping of water spring potential using four data mining models. Water Supply, 23(5), 1743-1759.

8.   Chapagain, P. S., Ghimire, M., & Shrestha, S. (2019). Status of natural springs in the Melamchi region of the Nepal Himalayas in the context of climate change. Environment, Development and Sustainability, 21, 263-280.

9.   Chowdary, V. M., Chakraborthy, D., Jeyaram, A., Murthy, Y. K., Sharma, J. R., & Dadhwal, V. K. (2013). Multi-criteria decision making approach for watershed prioritization using analytic hierarchy process technique and GIS. Water resources management, 27, 3555-3571.

10.   Saranya, T., & Saravanan, S. (2020). Groundwater potential zone mapping using analytical hierarchy process (AHP) and GIS for Kancheepuram District, Tamilnadu, India. *Modeling Earth Systems and Environment*, *6*(2), 1105-1122.

11.   Clark, C. D., & Wilson, C. (1994). Spatial analysis of lineaments. Computers & Geosciences, 20(7-8), 1237-1258.

12.   Danert, K., & Theis, S. (2017). Professional Management of Water Well Drilling Projects and Programmes Online Course 2018; Report for Course Participants. UNICEF-Skat Foundation Collaboration, 2019.

13.   Dinesh Kumar PK, Gopinath G, Seralathan P (2007) Application of remote sensing and GIS for the demarcation of groundwater potential zones of a river basin in Kerala, southwest cost of India.Int J Remote Sens 28(24):5583–5601

14.   Ettazarini, S. (2007). Groundwater potentiality index: a strategically conceived tool for water research in fractured aquifers. Environmental Geology, 52(3), 477-487.

15.   Foster, S. (2022). The key role for groundwater in urban water-supply security. Journal of Water and Climate Change, 13(10), 3566-3577.

16.   Ganapuram, S., Kumar, G. V., Krishna, I. M., Kahya, E., & Demirel, M. C. (2009). Mapping of groundwater potential zones in the Musi basin using remote sensing data and GIS. Advances in Engineering Software, 40(7), 506-518.

17.   Ghimire, M., Chapagain, P. S., & Shrestha, S. (2019). Mapping of groundwater spring potential zone using geospatial techniques in the Central Nepal Himalayas: a case example of Melamchi–Larke area. Journal of Earth System Science, 128(2), 26.

18.   Gnanachandrasamy, G., Zhou, Y., Bagyaraj, M., Venkatramanan, S., Ramkumar, T., & Wang, S. (2018). Remote sensing and GIS based groundwater potential zone mapping in Ariyalur District, Tamil Nadu. Journal of the Geological Society of India, 92, 484-490.

19.   Guru, B., Seshan, K., & Bera, S. (2017). Frequency ratio model for groundwater potential mapping and its sustainable management in cold desert, India. Journal of King Saud University-Science, 29(3), 333-347.

20.   Heim, A. (1939). Central Himalaya. Denkschr. Schweiz. Naturforsch. Ges., 73, 1-245.

21.   Hobbs WH (1904). Lineaments of the Atlantic border region. Geol. Soc. Am. Bull. 15:483-506.

22.   Hoque, S. F., Hope, R., Arif, S. T., Akhter, T., Naz, M., & Salehin, M. (2019). A social-ecological analysis of drinking water risks in coastal Bangladesh. Science of The Total Environment, 679, 23–34. https: //doi .org /10 .10 16/ j.s cit ote nv. 20 19.04.359.

23.   Islam, F., Tariq, A., Guluzade, R., Zhao, N., Shah, S. U., Ullah, M., ... & Aslam, M. (2023). Comparative analysis of GIS and RS based models for delineation of groundwater potential zone mapping. *Geomatics, Natural Hazards and Risk*, *14*(1), 2216852.

24.   Jha, M. K., Chowdary, V. M., & Chowdhury, A. (2010). Groundwater assessment in Salboni Block, West Bengal (India) using remote sensing, geographical information system and multi-criteria decision analysis techniques. Hydrogeology Journal, 18(7), 1713-1728.

25. Kebede, S. (2012). Groundwater in Ethiopia: features, numbers and opportunities. Springer Science & Business Media.

26. Khosravi, K., Panahi, M., & Tien Bui, D. (2018). Spatial prediction of groundwater spring potential mapping based on an adaptive neuro-fuzzy inference system and metaheuristic optimization. Hydrology and Earth System Sciences, 22(9), 4771-4792.

27. Kumar T, Gautam AK, Kumar T (2014) Appraising the accuracy of GIS multi-criteria decision making technique for delineation of groundwater potential zone. Water Resour Manage 28:4449–4466.

28. Kumar, R., Dwivedi, S.B., Gaur, S., 2021. A comparative study of machine learning and Fuzzy-AHP technique to groundwater potential mapping in the data-scarce region. Comput. Geosci. 155. https://doi.org/10.1016/j.cageo.2021.104855 104855.

29. Kumar, V., & Sen, S. (2018). Evaluation of spring discharge dynamics using recession curve analysis: a case study in data-scarce region, Lesser Himalayas, India. Sustainable Water Resources Management, 4, 539-557.

30. Li, P., Qian, H., & Wu, J. (2018). Conjunctive use of groundwater and surface water to reduce soil salinization in the Yinchuan Plain, North-West China. International Journal of Water Resources Development, 34(3), 337-353.

31. Machiwal, D., Jha, M. K., & Mal, B. C. (2011). Assessment of groundwater potential in a semi-arid region of India using remote sensing, GIS and MCDM techniques. Water resources management, 25, 1359-1386.

32. Magesh, N. S., Chandrasekar, N., & Soundranayagam, J. P. (2012). Delineation of groundwater potential zones in Theni district, Tamil Nadu, using remote sensing, GIS and MIF techniques. Geoscience frontiers, 3(2), 189-196.

33. Mahamuni, K., & Kulkarni, H. (2012). Groundwater resources and spring hydrogeology in South Sikkim, with special reference to climate change, climate change in Sikkim patterns, impacts and initiatives. Information and Public Relations Department, Government of Sikkim

34. Maupin, Molly A. Summary of estimated water use in the United States in 2015. No. 2018-3035. US Geological Survey, 2018.

35. Merh, S. S., & Vashi, N. M. (1965). Structure and metamorphism of the Ranikhet area of Almora District, Uttar Pradesh. Indian Mineralogist, 6, 55-66.

36. Moghaddam, D. D., Rezaei, M., Pourghasemi, H. R., Pourtaghie, Z. S., & Pradhan, B. (2015). Groundwater spring potential mapping using bivariate statistical model and GIS in the Taleghan watershed, Iran. Arabian Journal of Geosciences, 8, 913-929.

37. Muheeb MA, Rasheed AJ (2009) Evaluation of aquifers vulnerability to contamination in the Yarmouk river watershed, Jordan, based on DRASTIC method. Arab J Geosci 3:273–282

38. Muralitharan, J., & Palanivel, K. (2015). Groundwater targeting using remote sensing, geographical information system and analytical hierarchy process method in hard rock aquifer system, Karur district, Tamil Nadu, India. Earth Science Informatics, 8, 827-842.

39. Nag S 2005 Application of lineament density and hydrogeomorphology to delineate groundwater potential zones of Baghmundi block in Purulia district, West Bengal; J. Indian Soc. Remote Sens. 33(4) 521–529.

40. Upadhyay, R. K., Tripathi, G., Đurin, B., Šamanović, S., Cetl, V., Kishore, N., ... & Bhardwaj, V. (2023). Groundwater potential zone mapping in the Ghaggar River Basin, North-West India, using integrated remote sensing and GIS techniques. Water, 15(5), 961.

41. Naghibi, S. A., Pourghasemi, H. R., Pourtaghi, Z. S., & Rezaei, A. (2015). Groundwater qanat potential mapping using frequency ratio and Shannon's entropy models in the Moghan watershed, Iran. Earth Science Informatics, 8, 171-186.

42. Nampak, H., Pradhan, B., & Abd Manap, M. (2014). Application of GIS based data driven evidential belief function model to predict groundwater potential zonation. Journal of Hydrology, 513, 283-300.

43. National Groundwater Association. NGWA Groundwater Facts. Available online: https://www.ngwa.org/what-is-groundwater/About-groundwater/groundwater-facts (accessed on 3 February 2024).

44. Paul, S., & Roy, D. (2023). Geospatial modeling and analysis of groundwater stress-prone areas using GIS-based TOPSIS, VIKOR, and EDAS techniques in Murshidabad district, India. Modeling Earth Systems and Environment, 10(1), 121-141.

45. Pradhan, B. (2009). Groundwater potential zonation for basaltic watersheds using satellite remote sensing data and GIS techniques. Central European Journal of Geosciences, 1, 120-129.

46. Prasad Jha, M. K., Chowdhury, A., Chowdary, V. M., & Peiffer, S. (2007). Groundwater management and development by integrated remote sensing and geographic information systems: prospects and constraints. *Water resources management*, *21*, 427-467.

47. Prasad, R. K., Mondal, N. C., Banerjee, P., Nandakumar, M. V., & Singh, V. S. (2008). Deciphering potential groundwater zone in hard rock through the application of GIS. Environmental geology, 55, 467-475.

48. Rahmati, O., Nazari Samani, A., Mahdavi, M., Pourghasemi, H. R., & Zeinivand, H. (2015). Groundwater potential mapping at Kurdistan region of Iran using analytic hierarchy process and GIS. Arabian Journal of Geosciences, 8, 7059-7071.

49. Rahmati, O., Pourghasemi, H. R., & Melesse, A. M. (2016). Application of GIS-based data driven random forest and maximum entropy models for groundwater potential mapping: a case study at Mehran Region, Iran. Catena, 137, 360-372.

50. Rai, S. P. (1993) Hydrological and geomorphological studies of the Sya hidevi-Binsar Area, District Almora. Unpublished Ph D thesis, Kumaun University, Nainital, p 160.

51. Rai, S. P., Valdiya, K. S., & Rawat, J. S. (1998). Management of water resources: Spring sanctuaries. The Khulgad Project: An Experiment in Sustainable Development, Gyanodaya Prakashan, Nainital, India, 41-60.

52. Rajesh, J., Pande, C.B., Kadam, S.A., Gorantiwar, S.D., Shinde, M.G., 2021. Exploration of groundwater potential zones using analytical hierarchical process (AHP) approach in the Godavari River basin of Maharashtra in India. Appl Water Sci 11, 182. https:// doi.org/10.1007/s13201-021-01518-x

53. Rana, S., & Gupta, V. (2009). Watershed management in the indian himalayan region: issues and challenges. Proceedings of the World Environmental and Water Resources Congress; 2009. https://doi.org/10. 1061/41036(342)527

54. Ranjan, P., Pandey, P. K., & Pandey, V. (2023). Groundwater spring potential zonation using AHP and fuzzy-AHP in Eastern Himalayan region: Papum Pare district, Arunachal Pradesh, India. Environmental Science and Pollution Research, 31(7), 10317-10333.

55. Rao, N. S., Gugulothu, S., & Das, R. (2022). Deciphering artificial groundwater recharge suitability zones in the agricultural area of a river basin in Andhra Pradesh, India using geospatial techniques and analytical hierarchical process method. Catena, 212, 106085.

56. Rawat, J. S. (2010). Database management system for Khulgad WatershedKhulgad micro watershed, Kumaun Lesser Himalaya, Uttarakhand, India. *Current Science*, *98*(10), 1340–1348.

57. Rawat, J. S., & Rawat, G. (2020). Dying and dwindling of non-glacial fed rivers under climate change (a case study from the upper kosi watershed, central Himalaya, India). Geoecology of Landscape Dynamics, 53-74.

58. Rawat, S. S., Jose, P. G., Rai, S. P., & Hakhoo, N. (2018). spring sanctuary development: sustaining water security in the himalayan region in changing climate.

59. Shahid S, Nath SK, Ray J (2000) Groundwater potential modeling in softrock using a GIS. Int J Remote Sens 21:1919–1924.

60. Shekhar, S., & Pandey, A. C. (2015). Delineation of groundwater potential zone in hard rock terrain of India using remote sensing, geographical information system (GIS) and analytic hierarchy process (AHP) techniques. Geocarto International, 30(4), 402-421.

61. Sathiyamoorthy, M., Masilamani, U. S., Chadee, A. A., Golla, S. D., Aldagheiri, M., Sihag, P., ... & Martin, H. (2023). Sustainability of groundwater potential zones in coastal areas of Cuddalore District, Tamil Nadu, South India using integrated approach of remote sensing, GIS and AHP techniques. Sustainability, 15(6), 5339.

62. Srivastava, P. K., & Bhattacharya, A. K. (2006). Groundwater assessment through an integrated approach using remote sensing, GIS and resistivity techniques: a case study from a hard rock terrain. International Journal of Remote Sensing, 27(20), 4599-4620.

63. Tambe, S., Arrawatia, M. L., Bhutia, N. T., & Swaroop, B. (2011). Rapid, cost-effective and high-resolution assessment of climate-related vulnerability of rural communities of Sikkim Himalaya, India. Current Science, 101(2), 165–173.

64. Tariq, A., Ali, S., Basit, I., Jamil, A., Farmonov, N., Khorrami, B., ... & Hatamleh, W. A. (2023). Terrestrial and groundwater storage characteristics and their quantification in the Chitral (Pakistan) and Kabul (Afghanistan) river basins using GRACE/GRACE-FO satellite data. *Groundwater for Sustainable Development*, *23*, 100990.

65. Taylor, R. G., Scanlon, B., Döll, P., Rodell, M., Van Beek, R., Wada, Y., ... & Treidel, H. (2013). Ground water and climate change. Nature climate change, 3(4), 322-329.

66. U.N., 2023. The Sustainable Development Goals Report special edition. United Nations

67. Valdiya, K. S. (1980). The two intracrustal boundary thrusts of the Himalaya. Tectonophysics, 66(4), 323-348.

68. Waikar, M. L., & Nilawar, A. P. (2014). Identification of groundwater potential zone using remote sensing and GIS technique. International Journal of Innovative Research in Science, Engineering and Technology, 3(5), 12163-12174.

69. Wei, A., Li, D., Bai, X., Wang, R., Fu, X., & Yu, J. (2022). Application of machine learning to groundwater spring potential mapping using averaging, bagging, and boosting techniques. *Water Supply*, *22*(8), 6882-6894.

70. Yousefi, S., Sadhasivam, N., Pourghasemi, H. R., Nazarlou, H. G., Golkar, F., Tavangar, S., & Santosh, M. (2020). Groundwater spring potential assessment using new ensemble data mining techniques. Measurement, 157, 107652.

71. Aayog, N. I. T. I. "Inventory and revival of springs in the Himalayas for water security." Dept. of Science and Technology, Government of India, New Delhi (2017).

72. Hinton, J. C. (1996) "GIS and remote sensing integration for environmental applications." International Journal of Geographical Information Systems 10.7 877-890.

73. Zektser, I. S., & Everett, L. G. (2004). Groundwater resources of the world and their use.

74. Zhao, R., Fan, C., Arabameri, A., Santosh, M., Mohammad, L., & Mondal, I. (2024). Groundwater spring potential mapping: Assessment the contribution of hydrogeological factors. Advances in Space Research.

75. Mahato R, Bushi D, Nimasow G, Nimasow OD, Joshi RC (2022) AHP and GIS-based delineation of groundwater potential of Papum Pare District of Arunachal Pradesh, India. J Geol Soc India 98(1):102–112. https:// doi. org/ 10. 1007/ s12594- 022- 1936-y.

76. Saaty TL (1980) The analytic hierarchy process. McGraw-Hill, New York, p 287.

77. Goitsemang T, Das DM, Raul SK, Subudhi CR, Panigrahi B (2020) Assessment of groundwater potential in the Kalahandi District of Odisha (India) using remote sensing, geographic information system and analytical hierarchy process. J Indian Soc Remote Sens 48(12):1739–1753. https:// doi. org/ 10. 1007/ s12524- 020- 01188-3.18:21

78. Nijesh, P., Akpataku, K. V., Patel, A., Rai, P., & Rai, S. P. (2021). Spatial variability of hydrochemical characteristics and appraisal of water quality in stressed phreatic aquifer of Upper Ganga Plain, Uttar Pradesh, India. Environmental Earth Sciences, 80, 1-15.

79. Singh, A., Kumar, R., Kumar, R., Pippal, P. S., Sharma, P., & Sharma, A. (2024). Delineation of groundwater potential zone using geospatial tools and analytical hierarchy process (AHP) in the State of Uttarakhand, India. Advances in Space Research, 73(6), 2939-2954.

80. Roy, S. K., Hasan, M. M., Mondal, I., Akhter, J., Roy, S. K., Talukder, S., ... & Karuppannan, S. (2024). Empowered machine learning algorithm to identify sustainable groundwater potential zone map in Jashore District, Bangladesh. Groundwater for Sustainable Development, 25, 101168.

81. Zerouali, B., Bailek, N., Islam, A. R. M. T., Katipoğlu, O. M., Ayek, A. A. E., Santos, C. A. G., ... & Elbeltagi, A. (2024). Enhancing Groundwater Potential Zone Mapping with a Hybrid Analytical Method: The Case of semiarid basin. Groundwater for Sustainable Development, 101261.

82. Raj, S., Rawat, K. S., Singh, S. K., & Mishra, A. K. (2024). Groundwater potential zones identification and validation in Peninsular India. Geology, Ecology, and Landscapes, 8(1), 86-100.

83. Kom, K. P., Gurugnanam, B., & Sunitha, V. (2024). Delineation of groundwater potential zones using GIS and AHP techniques in Coimbatore district, South India. International Journal of Energy and Water Resources, 8(1), 85-109.

84. Pawar, U., Suppawimut, W., & Rathnayake, U. (2024). Mapping of groundwater potential zones in a drought prone Marathwada Region using frequency ratio and statistical index methods, India. *Results in Engineering*, *22*, 101994.

85. Patel, A., Rai, S. P., Puthiyottil, N., Singh, A. K., Noble, J., Singh, R., ... & Akpataku, K. V. (2024). Refining aquifer heterogeneity and understanding groundwater recharge sources in an intensively exploited agrarian dominated region of the Ganga Plain. Geoscience Frontiers, 15(4), 101808.

86. Doke AB, Zolekar RB, Patel H, Das S (2021) Geospatial mapping of groundwater potential zones using multicriteria decision-making AHP approach in a hardrock basaltic terrain in India. Ecol Indic127:1–16. https:// doi. org/ 10. 1016/j. ecoli nd. 2021. 107685.

87. Ghimire M, Chapagain PS, Shrestha S (2019) Mapping of groundwater spring potential zone using geospatial techniques in the Central Nepal Himalayas: a case example of Melamchi-Larke area. J Earth Syst Sci 128(2):1–24. https:// doi. org/ 10. 1007/ s12040- 018- 1048-7.